Circulating osteopontin per tumor volume as a prognostic biomarker for resectable intrahepatic cholangiocarcinoma

Kai-Qian Zhou[1,2#], Wei-Feng Liu[1,2,3#], Liu-Xiao Yang[1,2#], Yun-Fan Sun[1,2,4], Jie Hu[1,2,4], Fei-Yu Chen[1,2], Cheng Zhou[1,2], Xiang-Yu Zhang[1,2], Yuan-Fei Peng[1,2,4], Lei Yu[1,2,4], Jian Zhou[1,2,3,5], Jia Fan[1,2,3,5], Zheng Wang[1,2,4]

[1]Liver Cancer Institute, Zhongshan Hospital, Fudan University, Shanghai 200032, China; [2]Key Laboratory of Carcinogenesis and Cancer Invasion, Fudan University, Ministry of Education, Shanghai 200032, China; [3]Department of Hepatobiliary and Pancreatic Surgery, the Second Affiliated Hospital, Zhejiang University School of Medicine, Hangzhou 310009, China; [4]Department of Liver Surgery and Transplantation, Liver Cancer Institute, Zhongshan Hospital, [5]Institutes of Biomedical Sciences, Fudan University, Shanghai 200032, China

Contributions: (I) Conception and design: KQ Zhou, WF Liu, Z Wang; (II) Administrative support: J Zhou, J Fan; (III) Provision of study material or patients: LX Yang, YF Sun, J Hu; (IV) Collection and assembly of data: KQ Zhou, FY Chen, C Zhou, XY Zhang; (V) Data analysis and interpretation: KQ Zhou, YF Peng, L Yu; (VI) Manuscript writing: All authors; (VII) Final approval of manuscript: All authors.
[#]These authors contributed equally to this work.

Correspondence to: Zheng Wang. Liver Cancer Institute, Zhongshan Hospital, Fudan University, 180 Fenglin Road, Shanghai 200032, China. Email: wang.zheng@zs-hospital.sh.cn.

Background: The role of osteopontin (OPN) in intrahepatic cholangiocarcinoma (ICC) remains controversial. This study aimed to explore the prognostic value of OPN in patients with ICC undergoing curative resection.

Methods: Patients undergoing curative resection from 2005 to 2016 were identified for inclusion in this retrospective study. The expression level of OPN in tumors was measured in each of the 228 patients by immunohistochemistry. Circulating OPN in serum was tested in 124 patients by ELISA. Tumor volume was calculated according to preoperative imaging or operation record. Proliferation assay, wound healing assay, and invasion assay were performed to investigate the biological function.

Results: Low expression of OPN in tissue was associated with lymph node metastasis (P=0.009) and shorter overall survival (OS) (P=0.001). A low level of circulating OPN/volume was associated with multiple tumors (P<0.001), vascular invasion (P=0.027), visceral peritoneal perforation (P=0.001), and lymph node metastasis (P=0.002). It was also able to predict the invasive behavior, lymph node metastasis, and early recurrence with the area under the receiver operating curve (AUC) of being 0.719, 0.708 and 0.622 respectively. Patients with a low level of circulating OPN/volume had shorter OS (P=0.028) and disease-free survival (DFS) (P=0.004) and could benefit from adjuvant chemotherapy (P=0.011). Compared with negative controlled cells, ICC cell lines, which expressed more OPN, showed a decelerated proliferation rate, the weaker ability of migration and invasion, while the opposite was true for the cells expressed less OPN. *MMP1*, *MMP10*, and *CXCR4* were negatively regulated by OPN.

Conclusions: A low level of circulating OPN/volume could indicate aggressive characteristics, along with poor prognosis and efficacy of adjuvant chemotherapy in ICC patients. Over expression of OPN may inhibit phenotypes facilitating ICC metastasis by negatively regulating *MMP1*, *MMP10*, and *CXCR4*.

Keywords: Intrahepatic cholangiocarcinoma (ICC); osteopontin (OPN); prognosis

Introduction

Intrahepatic cholangiocarcinoma (ICC) is a subtype of cholangiocarcinoma, accounting for approximately 10% of the total reported cases (1). ICC can arise from biliary epithelium in any portion of the intrahepatic biliary system, from ductules to segmental bile ducts proximal to the bifurcation of the hepatic ducts (2). Over the last few decades, the incidence of ICC worldwide has been increasing (3,4), leading to a concomitant rise in the mortality rate (5,6). The 1- and 2-year survival rates following diagnosis are only 24.5% and 12.8% respectively (7) and resection remains the primary effective first-line treatment for ICC; median survival time can reach above 30 months (8,9) when the tumor is completely removed. Even so, quite a number of patients experience recurrence or died shortly after the aggressive resection. It still remains unclear how to select the patients who would optimally benefit from surgery. Invasive and metastatic characteristics of ICC are usually considered as risk factors for recurrence and long-term survival (10-15). However, the confirmation of these characteristics relies on pathological examination. Therefore, a suitable preoperative testing method is in need to judge the invasive and metastatic ability of ICC and assess the survival benefit of resection, so as to help develop a treatment strategy.

Osteopontin (OPN) is a glycosylated phosphoprotein encoded by the gene *SPP1* (secreted phosphoprotein 1). It can be found in a variety of cells, tissues and body fluids. It is involved in diverse biological processes such as biomineralization, bone remodeling, immune function, chemotaxis, cell survival, and tumorigenesis via receptors involving integrin and CD44. A large number of human tumor types express OPN, including hepatocellular carcinoma (HCC) and ICC, both of which are primary liver cancers. The relationship between OPN and HCC has drawn researchers' attention and has been studied intensively. It is believed that OPN promotes the progression of HCC in different ways, such as apoptosis inhibition (16), extracellular matrix (ECM) degeneration (17), stemness enhancement (18), epithelial-mesenchymal transition (EMT) (19,20) and migration (21). With regards to ICC, whether OPN is able to provide early detection of invasive, and metastatic behavior remains unclear. The studies on the role of OPN in ICC are limited and controversial. Terashi *et al.* (22) and Iguchi *et al.* (23) reported that decreased expression of OPN in the tissue was considered to be an indicator for aggressive phenotype and shorter survival;

whereas Zheng *et al.* (24) found that elevated OPN in the serum was associated with poor prognosis after resection.

Therefore, this study aims to investigate the clinical value of OPN in predicting prognosis and developing treatment strategy and explore the possible mechanisms of the function of OPN.

Methods

Patients and specimens

All patients enrolled in this study had no history of malignant tumor or anti-tumor treatment, had undergone curative resection with a clear surgical margin, and had a pathological diagnosis of ICC. Archival specimens from 2005 to 2016 were obtained from patients at Zhongshan Hospital, Fudan University after informed consent. Eighty-five cases of frozen tissue, 228 cases of formalin-fixed and paraffin-embedded (FFPE) tissue, and 124 cases of preoperative serum were selected based on complete clinicopathological and survival data for the patients. Forty-one patients had frozen tissue and serum at the same time. This study was approved by the ethics committee at Zhongshan Hospital.

Reverse transcription and quantitative polymerase chain reaction

RNA was extracted by TRIzol (Invitrogen), followed by reverse transcription with a High Capacity cDNA Reverse Transcription Kit (Applied Biosystems). qPCR and PCR array (Human Tumor Metastasis Array Plates, Taqman) were conducted using 7900HT Fast Real-Time PCR (Applied Biosystems). The primers used in qPCR were synthesized according to the following sequence listed in PrimerBank (25): *GAPDH* (378404907c1), *SPP1* (352962175c1), *CXCR4* (56790928c1), *MMP1* (225543092c1), *MMP10* (296080749c1). Gene expression was calculated by the $2^{-\Delta\Delta Ct}$ algorithm normalized to *GAPDH*.

Evaluation of serum markers

Frozen serums derived from ICC patients and healthy subjects were used for the double-blinded quantitative detection of certain markers. Concentrations of OPN were calculated using a Human osteopontin/OPN ELISA Kit (Multi Science, China) according to the manufacturer's
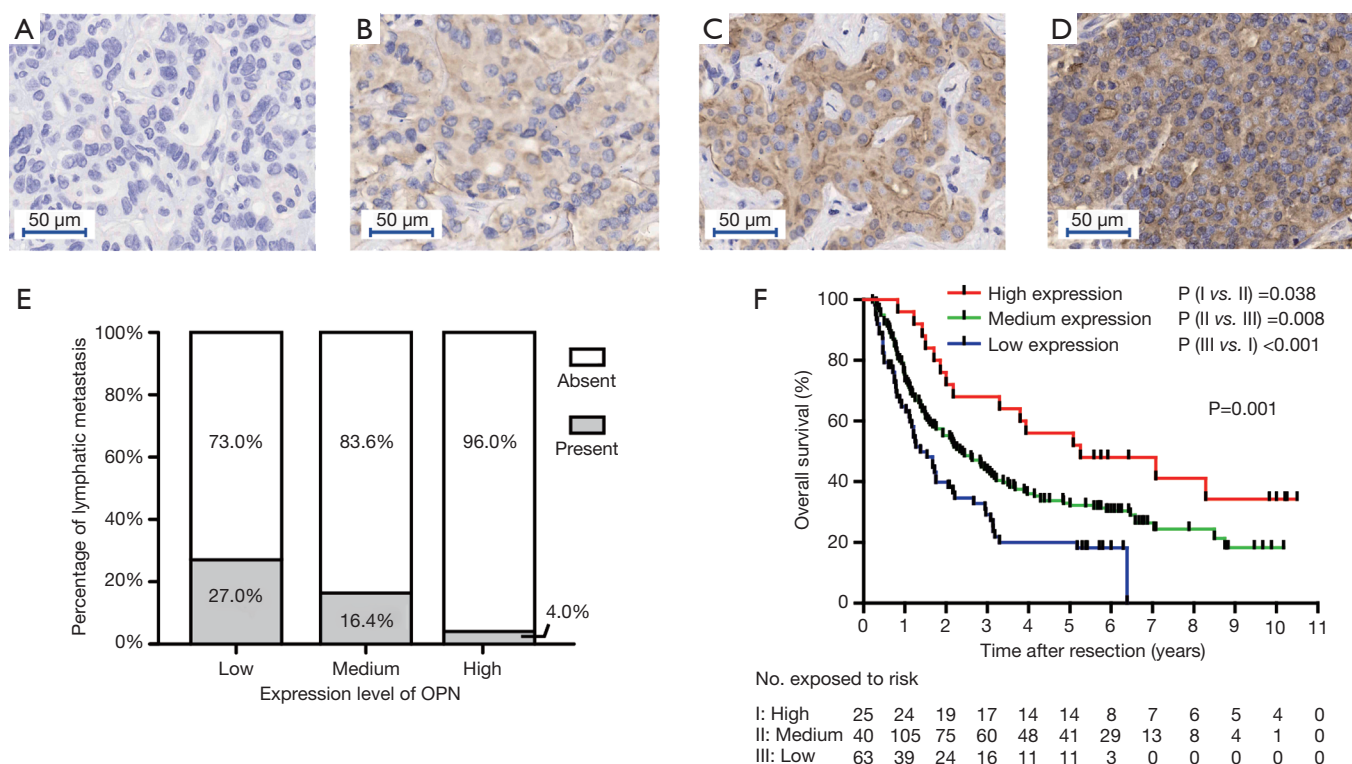
Figure 1 The association of OPN in tumor tissue with prognosis. (A,B,C,D) Immunohistochemical staining of OPN in ICC tissues. According to the intensity and extent of staining, expression levels of OPN were grouped into negative (A), weak (B), medium (C), and strong (D); (E) the incidence of lymph node metastasis decreased as the expression level of OPN increased (P=0.009, Jonckheere-Terpstra analysis); (F) survival analysis. The expression level of OPN was significantly associated with overall survival (n=228, P=0.001, log-rank statistics). OPN, osteopontin; ICC, intrahepatic cholangiocarcinoma.

protocol. Each sample was tested in triplicate. Expression of CEA and CA19-9 was determined by Cobas E602 (R&D) at the Department of Laboratory Medicine in Zhongshan Hospital.

Calculation of tumor volume

Tumor volume measurement was performed by a radiologist if patients' preoperative CT was accessible (26). Otherwise, tumor volume was calculated using the formula ($4/3 \times \pi \times$ length $\times$ width $\times$ height), according to the surgery record (27). Total tumor volume was the sum of the volumes of total lesions in one patient. Serum OPN/volume was defined as the ratio of serum OPN to total tumor volume (28).

Immunohistochemistry analysis

FFPE blocks were used to construct tissue microarrays (TMA), as described previously (29). Duplicates of cylinders

away from the necrotic and hemorrhagic area in the tumor were included in each case to ensure reproducibility (Shanghai Biochip Co., Ltd., Shanghai, China). TMA slides were incubated with polyclonal OPN antibody (22952-1-AP, Proteintech, China) at a 1:200 dilution. The staining pattern was semi-quantitatively evaluated by two pathologists (LL Chen, and M Du). IHC results of OPN were described by the sum of intensity score (negative =0, weak =1, moderate =2 and strong =3, *Figure 1A,B,C,D*) and percentage score (0%=0, 0–30%=1, 30–60%=2, 60–100%=3) (30). A score of 0–2 was classified as low expression, a score of 3–5 was classified as medium expression, and a score of 6 was classified as high expression.

Cell culture and transfection

Six cell lines were adopted in this study, including four human ICC cell lines (RBE, CCLPI, HCCC9810 and HuCCT1), one human hepatocyte cell line (ChangLiver)

and one human intrahepatic bile duct cell line (HIBEpic). Chang Liver was preserved at the Liver Cancer Institute, Fudan University. CCLPI and HuCCT1 were provided by Dr. Wang from the Institutes of Biomedical Sciences of Fudan University. RBE and HCCC9810 were provided by the Shanghai Cell Bank, Chinese Academy of Sciences. HIBEpic was purchased from ScienCell Research Laboratories (Carlsbad, CA, USA). Cells were maintained in RPMI-1640 culture medium (GIBCO) supplemented with 10% FBS (GIBCO), 100 IU/mL penicillin, and 100 mg/mL streptomycin (GIBCO). Full-length OPN and cDNAs were cloned into lentiviral vectors pCDH-CMV-MCS-EF1. These vectors, together with the empty vectors, were used to transfect both HCCC9810 and HuCCT1. Lentiviral vectors containing *SPP1* shRNA or non-target shRNA control were constructed using GenePharma (GenePharma, Shanghai, China). These vectors were used to transfect HCCC9810 and RBE.

Proliferation and migration assay

Cellular function assays, which are proliferation and migration assays, were measured using an automated time-lapse phase-contrast microscope system named Cell-IQ (Chip-Man Technologies, Finland) (28). This system provides a stable atmosphere (5% CO_2, 20% O_2, and 75% NO_2) and temperature of 37 ℃. The monitoring of cellular proliferation started after seeding the 24-well plate (Corning) at the density of 3,000 cells per well for 12 h. The monitoring of cellular migration began immediately after making a cross-directional scratch to the confluent cell layer at the 24-well plate with a pipette tip. The images were taken every full hour for 36 h. Cell number was estimated from images by Cell-IQ Analyser (version 2.2.1, Chip-Man Technologies) software. The velocity of migration was presented as the ratio of the cleaned area by ImageJ software (ImageJ 1.50 s, Wayne Rasband, National Institutes of Health, USA).

Transwell invasion assay

Cellular invasion ability was evaluated by Matrigel Transwell assays. Each Transwell insert was coated with Matrigel (BD) diluted in medium (1:8, 80 μL). Then, $1×10^5$ cells were plated into the Transwell inserts with RPMI-1640 medium. Next, 600 μL medium containing 10% fetal bovine serum (FBS) was injected into the lower chamber. Invaded cells were fixed and dyed after incubating for 48 h.

Cell numbers were counted as the average number in five random high magnification fields. Assays were performed in triplicate.

Statistical methods

Student's *t*-test or Mann-Whitney test was used to determine the differences between the two groups. Kaplan-Meier analysis was used to measure overall survival (OS) and disease-free survival (DFS). OS was the duration time of the interval from resection to death or latest follow-up. DFS was the duration time of the interval from resection to recurrence of ICC or death or last follow-up. Early recurrence was defined as recurrence occurring within 2 years after resection (31). Variables associated with OS were identified using Cox proportional hazards regression model. Prognostic factors verified in the univariate analysis were further subjected to multivariate Cox regression analysis in an enter method. One-way ANVOA or Kruskal-Wallis test was performed to determine certain clinicopathological data associated with OPN expression. Jonckheere-Terpstra was then undertaken to detect whether there was a priori ordering of the clinicopathological factor along with the enhancement of OPN expression. A 2-tailed P<0.05 was considered significant. Statistical analyses and graphs were generated using GraphPad Prism (version 5.01, GraphPad Software), SPSS (version 19.0, IBM), MedCalc (version 10.4.7.0, MedCalc Software) and X-tile (version 3.5.0, Yale University).

Results

Prognosis value of OPN in tumor tissue

TMAs comprising 228 cases were evaluated for the clinical value and the expression level of OPN in tumor tissue. Patients were divided into OPN low, medium, and high expression groups according to their IHC score. There were 63, 140, and 25 cases in these groups respectively.

The association with tissue OPN and clinicopathological characteristics was compared. It was found that lymph node metastasis (P=0.031) and Edmondson's grade (P=0.011) were significantly different among OPN expression subgroups (*Table S1*). Jonckheere-Terpstra analysis revealed that the incidence of lymph node metastasis decreased as the expression level of OPN increased (P=0.009, *Figure 1E*), while Edmondson's grade did not have an ordering with the change of OPN.
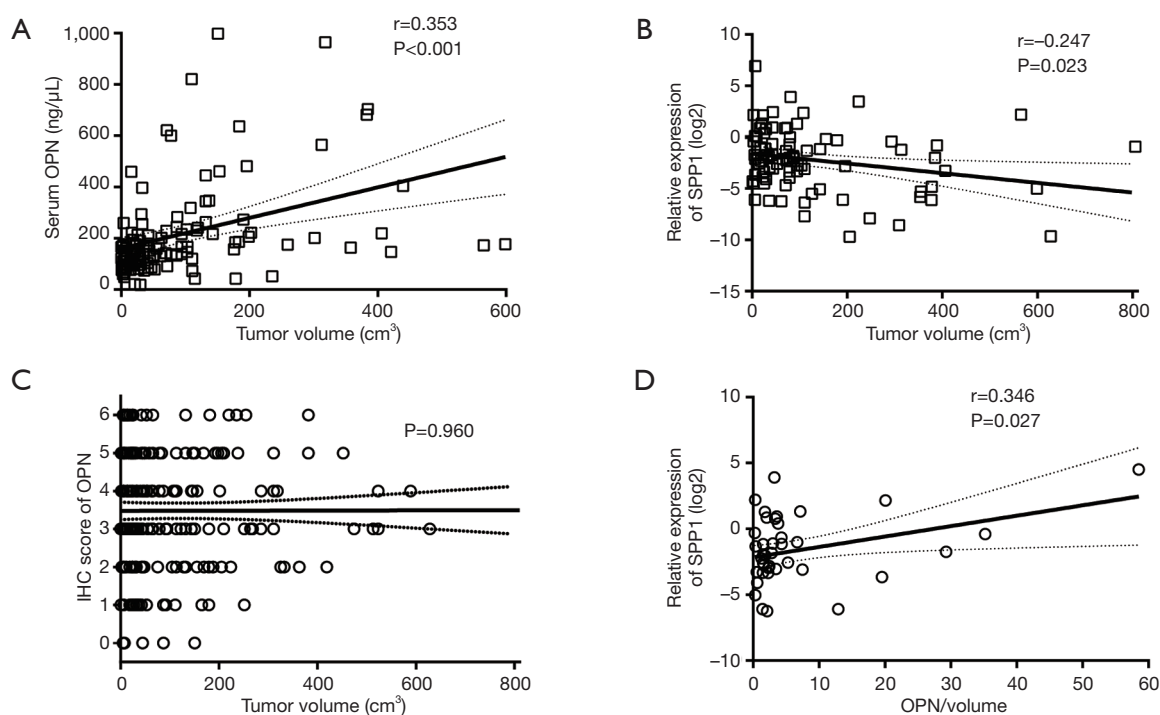
586

Zhou et al. Circulating OPN/volume in ICC

Figure 2 Relationship between OPN level and tumor volume. (A) Correlation between serum OPN and tumor volume (n=124, r=0.353, P<0.001); (B) correlation between tissue *SPP1*-mRNA and tumor volume (n=85, r=−0.247, P=0.023); (C) correlation between tissue OPN and tumor volume (n=228, P=0.960); (D) correlation between circulating OPN/volume and local *SPP1*-mRNA (n=41, r=0.346, P=0.027). OPN, osteopontin.

Remarkably, patients with a higher OPN expression level had better OS than patients in the median and low expression groups. The median survival of high, medium and low expression groups were 63.0, 28.7, and 16.5 months respectively (P=0.001, *Figure 1F*). Univariate analysis showed that multiple tumors, largest diameter, lymph node metastasis, CA19-9, and OPN were significantly correlated with OS. All five these clinicopathological characteristics were then tested in Cox's multivariate proportional hazards model. The results indicated that multiple tumors, largest diameter, lymph node metastasis, and low level of OPN expression were independent risk factors for OS (*Table S2*).

The relationship between serum OPN level and OPN in tumor tissue

We noticed that it was preoperative serum OPN (n=124, P<0.001, r=0.353, *Figure 2A*), rather than *SPP1*-mRNA (n=85, P=0.023, r=−0.247, *Figure 2B*) or OPN (n=228, P=0.960, *Figure 2C*) in tissue, that positively correlated with tumor volume. Considering that the larger ICC was

the more serum OPN, there would be, the size of the ICC might cover up the intrinsic effect of serum OPN. Therefore, we adjusted the serum OPN by tumor size, which was accomplished by dividing the OPN concentration by total tumor volume (OPN/volume) (27,28).

In 41 patients, frozen tissue and serum specimen were accessible at the same time. Before the adjustment of tumor size, *SPP1*-mRNA in the tissue was not correlated with serum OPN (n=41, P=0.737, *Figure S1A*). After the adjustment, patients with less *SPP1*-mRNA in the tissue had a lower level of circulating OPN/volume (n=41, P=0.043, *Figure S1B*), and circulating OPN/volume was positively correlated with local *SPP1*-mRNA (n=41, P=0.027, r=0.346, *Figure 2D*).

The association of circulating OPN/volume with clinicopathological characteristics and prognosis

The median circulating OPN/volume was 2.9 ng/mL/cm^3 (quartiles 1.4–6.6), and the mean ratio was 9.6±26.3 ng/mL/cm^3. A total of 124 patients were then separated into two groups

Table 1 Clinical characteristics of 124 ICC patients according to circulating OPN/volume

Clinicopathological factors	Circulating OPN/volume level		P value
	Low	High	
All cases	62	62	
Gender, male vs. female	33:29	35:27	0.718
Age, years, ≥60 vs. <60	31:31	38:24	0.206
Tumor number, multiple vs. solitary	24:38	7:55	<0.001*
Vascular invasion, present vs. absent	18:44	8:54	0.027*
Visceral peritoneal perforation, yes vs. no	11:51	0:62	0.001*
Lymph node metastasis, present vs. absent	15:47	3:59	0.002*
Edmondson's grade, III-IV vs. I-II	41:21	41:21	1.000
Liver cirrhosis, with vs. without	14:48	14:48	1.000
HBsAg, positive vs. negative	22:40	22:40	1.000
TB, μmol/L, >20.4 vs. ≤20.4	5:57	3:59	0.715
ALB, g/L, <35 vs. ≥35	58:4	58:4	1.000
ALT, U/L, >50 vs. ≤50	7:55	12:50	0.213
γ-GT, U/L, >60 vs. ≤60	30:32	22:40	0.145
CEA, ng/mL, >5 vs. ≤5	24:38	10:52	0.005*
CA19-9, U/mL, >37 vs. ≤37	37:25	31:31	0.279
TNM stage, III vs. II vs. I	20:20:22	4:14:44	<0.001*
Adjuvant TACE, yes vs. no	12:50	7:55	0.213
Adjuvant chemotherapy, yes vs. no	12:50	10:52	0.638
Adjuvant radiotherapy, yes vs. no	5:57	4:58	0.729

Analysis were performed using Cox proportional hazards model. *, P<0.05 by the Chi-square test. HBsAg, hepatitis B surface antigen; TB, total bilirubin; ALB, albumin; ALT, alanine aminotransferase; γ-GT, γ-glutamyl-transferase; CEA, carcinoembryonic antigen; CA19-9, carbohydrate antigen 19-9; TACE, transhepatic arterial chemotherapy and embolization; OPN, osteopontin; ICC, intrahepatic cholangiocarcinoma.

using the median ratio as the cutoff point. The high level group's (n=62) ratio was no less than 2.9 ng/mL/cm^3, and the low level group's (n=62) concentration was lower than 2.9 ng/mL/cm^3.

A low level of circulating OPN/volume was significantly associated with abnormal CEA (P=0.005), advanced Tumor, Nodes, Metastasis (TNM) stage (P<0.001), lymph node metastasis (P=0.002), along with invasive behavior (32) determined by multiple tumors (P<0.001), vascular invasion (P=0.027), and visceral peritoneal perforation (P=0.001) (*Table 1*).

Median follow-up time was 31.4 months. The 1- and 3-year cumulative proportions were 81.9% and 53.9% respectively, for OS, and 59.3% and 29.3%, respectively,

for DFS. Patients in the low OPN/volume group showed shorter OS (median, 31.5 months vs. no reached, P=0.028) and DFS (median, 11.6 vs. 25.7 months, P=0.004) than those in the high group (*Figure 3A,B*). Univariate analysis revealed that multiple tumors, largest diameter, vascular invasion, visceral peritoneal perforation, lymph node metastasis, γ-GT, CEA, and circulating OPN were significantly correlated with both OS and DFS (*Table 2*).

Predictive role of circulating OPN/volume on invasive behavior, lymph node metastasis and early recurrence

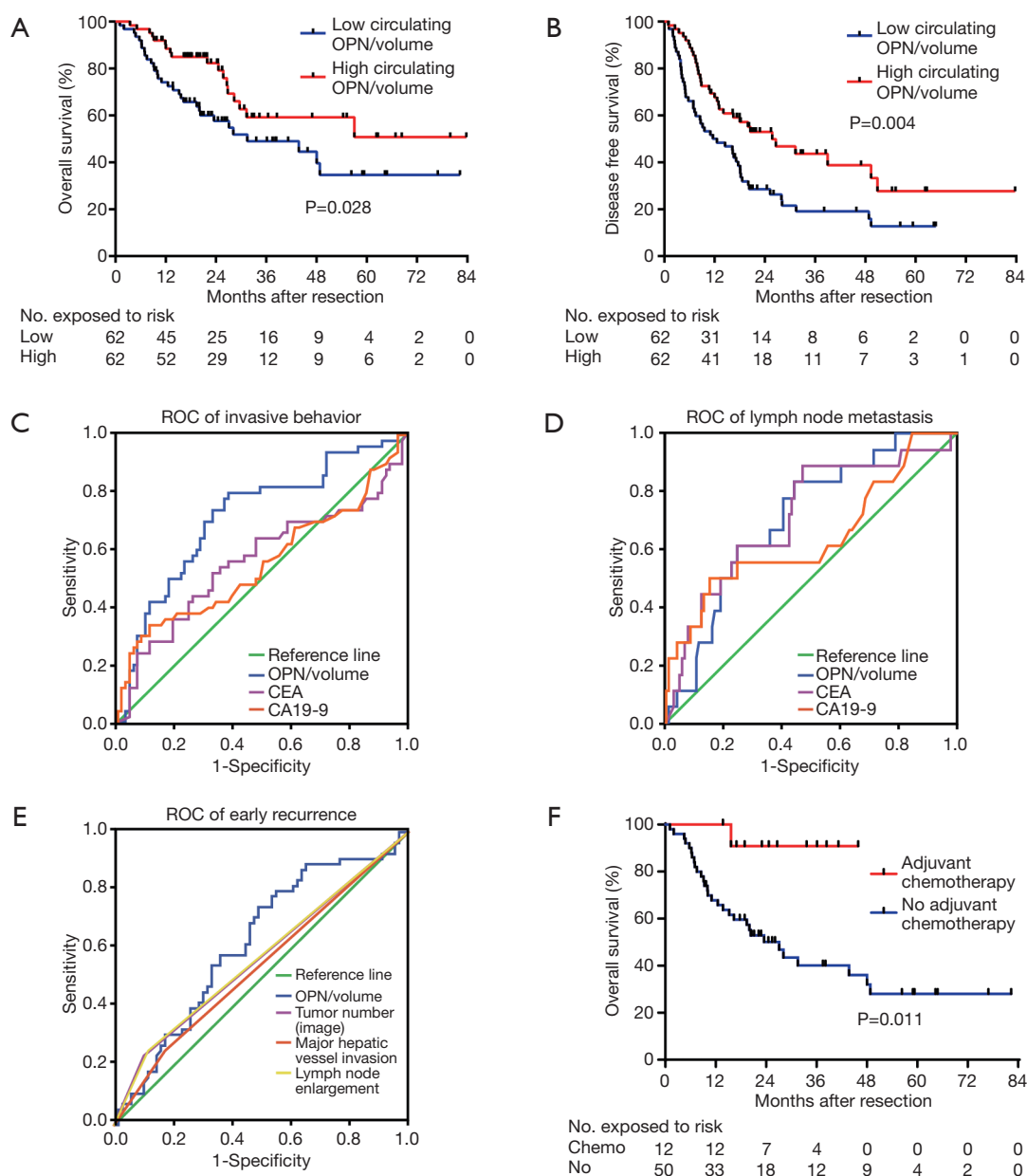Circulating OPN/volume was associated with invasive

Figure 3 The clinical value of circulating OPN per tumor volume. (A) Overall survival curve for high (red, n=62) and low (blue, n =62) group of circulating OPN/volume. The survival rates at 1 and 3 years were 90.0% and 57.8% respectively, in the high group, and 74.0% and 49.3% respectively, in the low group (P=0.028); (B) the disease-free survival curve for high and low circulating OPN/volume group. The survival rates at 1 and 3 years were 68.9% and 41.1% respectively, in the high group; and 50.0% and 19.1% respectively, in the low group (P=0.004); (C) ROC curve for OPN/volume (AUC 0.719; 95% CI, 0.630–0.796), CEA (AUC 0.553; 95% CI, 0.461–0.643), and CA19-9 (AUC 0.561; 95% CI, 0.469–0.650) in predicting invasive behavior in 124 ICC patients; (D) ROC curve for OPN/volume (AUC 0.708; 95% CI, 0.619–0.786), CEA (AUC 0.640; 95% CI, 0.549–0.725), and CA19-9 (AUC 0.712; 95% CI, 0.624–0.790) in predicting lymph node metastasis; (E) ROC curve for OPN/volume (AUC 0.622; 95% CI, 0.530–0.707), major hepatic vessel invasion (AUC 0.540; 95% CI, 0.449–0.630), lymph node enlargement (AUC 0.569; 95% CI, 0.477–0.658), and multiple tumors (AUC 0.567; 95% CI, 0.476–0.656) as indicated in the image in predicting early recurrence; (F) overall survival curve for the use of adjuvant chemotherapy (red, n=12) or not (blue, n=50) in patients with a low level of circulating OPN/volume. OPN, osteopontin.

Table 2 Univariate for OS and DFS in 124 cases of ICC after resection

Variables	n	Overall survival			Disease-free survival		
		HR	95% CI	P	HR	95% CI	P
Gender (male)	68	2.23	1.22–4.10	0.010*	1.22	0.79–1.88	0.364
Age ≥60	69	1.14	0.65–2.00	0.659	0.79	0.52–1.22	0.286
Multiple tumors	31	2.64	1.48–4.70	0.001*	2.23	1.40–3.53	0.001*
Largest diameter >5 cm	59	2.47	1.37–4.45	0.003*	1.94	1.26–2.99	0.003*
Incomplete tumor capsule	10	0.84	0.30–2.33	0.731	0.87	0.40–1.88	0.718
Visceral peritoneal perforation	11	4.75	2.19–10.33	<0.001*	3.40	1.77–6.55	<0.001*
Vascular invasion	26	1.95	1.03–3.69	0.040*	1.99	1.21–3.28	0.007*
Lymph node metastasis	18	3.08	1.54–6.18	0.002*	3.54	2.04–6.13	<0.001*
Edmondson grades III/IV	82	1.54	0.83–2.86	0.166	1.42	0.89–2.27	0.141
Liver cirrhosis	28	0.88	0.45–1.70	0.704	0.83	0.49–1.39	0.473
Child-Pugh B or C	2	0.42	0.10–1.77	0.239	0.84	0.21–3.43	0.806
HBsAg positive	44	0.89	0.49–1.61	0.696	1.01	0.65–1.58	0.958
TB >20.4 U/L	8	2.59	1.09–6.11	0.030*	1.14	0.50–2.62	0.760
ALB ≥35 g/L	116	0.73	0.26–2.05	0.554	0.85	0.39–1.84	0.674
ALT >40 U/L	19	1.65	0.86–3.16	0.135	1.44	0.84–2.45	0.182
γ-GT >60 U/L	52	1.78	1.01–3.13	0.045*	1.75	1.14–2.69	0.011*
CEA >5 ng/mL	34	2.24	1.26–3.96	0.006*	1.85	1.17–2.92	0.008*
CA19-9 >37 U/mL	68	1.24	0.70–2.18	0.466	1.90	1.22–2.97	0.005*
Serum OPN/volume	62	0.53	0.29–0.94	0.030*	0.53	0.34–0.82	0.004*
Adjuvant TACE	19	1.21	0.59–2.49	0.609	1.08	0.60–1.96	0.792
Adjuvant chemotherapy	22	0.21	0.05–0.87	0.031*	0.85	0.47–1.54	0.583
Adjuvant radiotherapy	9	1.06	0.38–2.94	0.917	1.08	0.50–2.35	0.844

Analysis were performed using Cox proportional hazards model. *, P<0.05 by the Cox regression test. HBsAg, hepatitis B surface antigen; TB, total bilirubin; ALB, albumin; ALT, alanine aminotransferase; γ-GT, γ-glutamyl-transferase; CEA, carcinoembryonic antigen; CA19-9, carbohydrate antigen 19-9; TACE, transhepatic arterial chemotherapy and embolization. OS, overall survival; DFS, disease-free survival; ICC, intrahepatic cholangiocarcinoma.

and metastatic characteristics. Therefore, we explored its predictive value one step further. According to ROC curves, circulating OPN/volume was able to predict multiple tumors (AUC 0.710; 95% CI, 0.621–0.788, *Figure S2A*), vascular invasion (AUC 0.670; 95% CI, 0.580–0.751, *Figure S2B*), and visceral peritoneal perforation (AUC 0.737; 95% CI, 0.650–0.812, *Figure S2C*). Using circulating OPN/volume in predicting invasive behavior (AUC 0.719; 95% CI, 0.630–0.796) was better than CEA (P=0.015) and CA19-9 (P=0.027) (*Figure 3C*). Circulating OPN/volume was also able to predict lymph node metastasis (AUC 0.708; 95%

CI, 0.619–0.786) and was no worse than CEA (P=0.508) or CA19-9 (P=0.960) (*Figure 3D*).

The calculation of OPN/volume relied on preoperative imaging, which included the information of tumor number, major hepatic vessel invasion, and lymph node enlargement. These factors are natural predictors of aggressive behavior. According to the ROC curves, OPN/volume was able to predict early recurrence after resection (AUC 0.622; 95% CI, 0.530–0.707, *Figure 3E*). However, major hepatic vessel invasion (AUC 0.540; 95% CI, 0.449–0.630), lymph node enlargement (AUC 0.569; 95% CI, 0.477–0.658) and

590

Zhou et al. Circulating OPN/volume in ICC

multiple tumors (AUC 0.567; 95% CI, 0.476–0.656), as indicated in the image, failed to predict early recurrence (*Figure 3E*).

The correlation between circulating OPN/volume and efficacy of adjuvant therapy

The number of patients receiving adjuvant transhepatic arterial chemotherapy and embolization (TACE), chemotherapy, and radiotherapy in the serum cohort (n=124) were 19, 22, and 9 respectively. In this study, adjuvant chemotherapy referred to as fluoropyrimidine-base or gemcitabine-based chemotherapy. The distribution of adjuvant therapy was similar between the low and high group of OPN/volume (*Table 1*). According to the univariate analysis, adjuvant chemotherapy improved OS (HR 0.210; 95% CI, 0.05–0.87, P=0.031) but not DFS, while neither TACE nor radiotherapy had influence on survival (*Table 2*).

To explore whether OPN/volume helpful in developing a postoperative treatment plan, the subgroup analyses of OS were performed. For patients with a low level of OPN/volume, the preventive use of chemotherapeutic drugs after resection correlated with better OS than the absence of use (median time not reached *vs.* 27.1 months, P=0.011, *Figure 3F*). While for those with a high level of OPN/volume, chemotherapy did not influence OS (P=0.545). Both TACE and radiotherapy failed to show a survival benefit in the subgroup analyses.

Over expression of OPN inhibits cell proliferation and invasion in vitro

ICC cell lines (RBE, CCLPI, HCCC9810, and HuCCT1) expressed less SPP1-mRNA, and OPN, than a normal intrahepatic bile epithelium cell line, HIBEpic (*Figure 4A*).

Expression levels of OPN (encoded by *SPP1*) in stably transfected ICC cell lines (RBE-shRNA-*SPP1*, RBE-shRNA-NC; HCCC9810-shRNA-*SPP1*, HCCC9810-shRNA-NC; HCCC9810-*SPP1*, HCCC9810-NC; HuCCT1-NC, HuCCT1-*SPP1*) were confirmed by quantitative real-time PCR (qRT-PCR) and western blot (*Figure S3*).

Cell proliferation rates of HCCC9810-*SPP1* and HuCCT1-*SPP1* were significantly lower than HCCC9810-NC and HuCCT1-NC cells during 48-hour observations (P<0.01, *Figure 4B*). RBE-shRNA-*SPP1* and HCCC 9810-shRNA-*SPP1* had faster proliferation rates than their negative controls. According to wound-healing migration

assays, microscopic examination at 36 h displayed a significant delay in the wound closure rate of HCCC9810-*SPP1* and HuCCT1-*SPP1* compared with their negative controls (*Figure 4C*); while the RBE-shRNA-*SPP1*'s and HCCC9810-shRNA-*SPP1*'s wound closure rates were more advanced than their control cells. Transwell invasion assay showed that the number of invaded cells was larger in the OPN down-regulated cells and smaller in the up-regulated cells (*Figure 4D*).

Metastasis associated genes influenced by OPN

Four gene-edited HCCC9810 cell lines (HCCC9810-shRNA-*SPP1*, HCCC9810-shRNA-NC, HCCC9810-*SPP1*, and HCCC9810-NC) were used to screen potential tumor metastasis associated genes caused by the expression of OPN (encoded by *SPP1*). The results of PCR array showed that the expression levels of 13 genes, which were *ITGB3*, *MMP1*, *LAMB1*, *MMP10*, *CXCR4*, *RBL2*, *ETV4*, *MTSS1*, *IL1B*, *KISS1*, *CDH1*, *MCAM*, and *MMP9*, decreased due to the up regulation of OPN [fold change (FC) <0.5, *Figure 5A*]. Furthermore, higher expression levels of *MMP10*, *CXCR4*, *MMP3*, and *MMP1* were seen following the down regulation of OPN (FC >2, *Figure 5B*). In summary, *MMP10*, *CXCR4*, and *MMP1* were potential metastasis-associated genes influenced by OPN.

To validate the results of the PCR array, qPCR was then taken repeatedly. RBE-shRNA-*SPP1* and HCCC9810-shRNA-*SPP1* had higher expression levels of *MMP10*, *CXCR4*, and *MMP1* than negative controls (*Figure 5C*); while HCCC9810-*SPP1* and HuCCT1-*SPP1* expressed less *MMP10*, *CXCR4*, and *MMP1* than NC cells (*Figure 5D*).

Discussion

The continuously increasing morbidity of ICC demands a deeper understanding of this lethal disease. Predicting the prognosis before the operation is of great value. It is beneficial not only to select suitable patients for resection but also to develop a comprehensive treatment plan as early as possible. In this study, a low level of circulating OPN/volume was found to be able to predict early recurrence, discriminate patients with shorter DFS and OS, and indicate the efficacy of adjuvant chemotherapy. The index could also predict aggressive characteristics including multiple tumors, vascular invasion, visceral peritoneal perforation, and lymph node metastasis. Tissue OPN per section showed similar
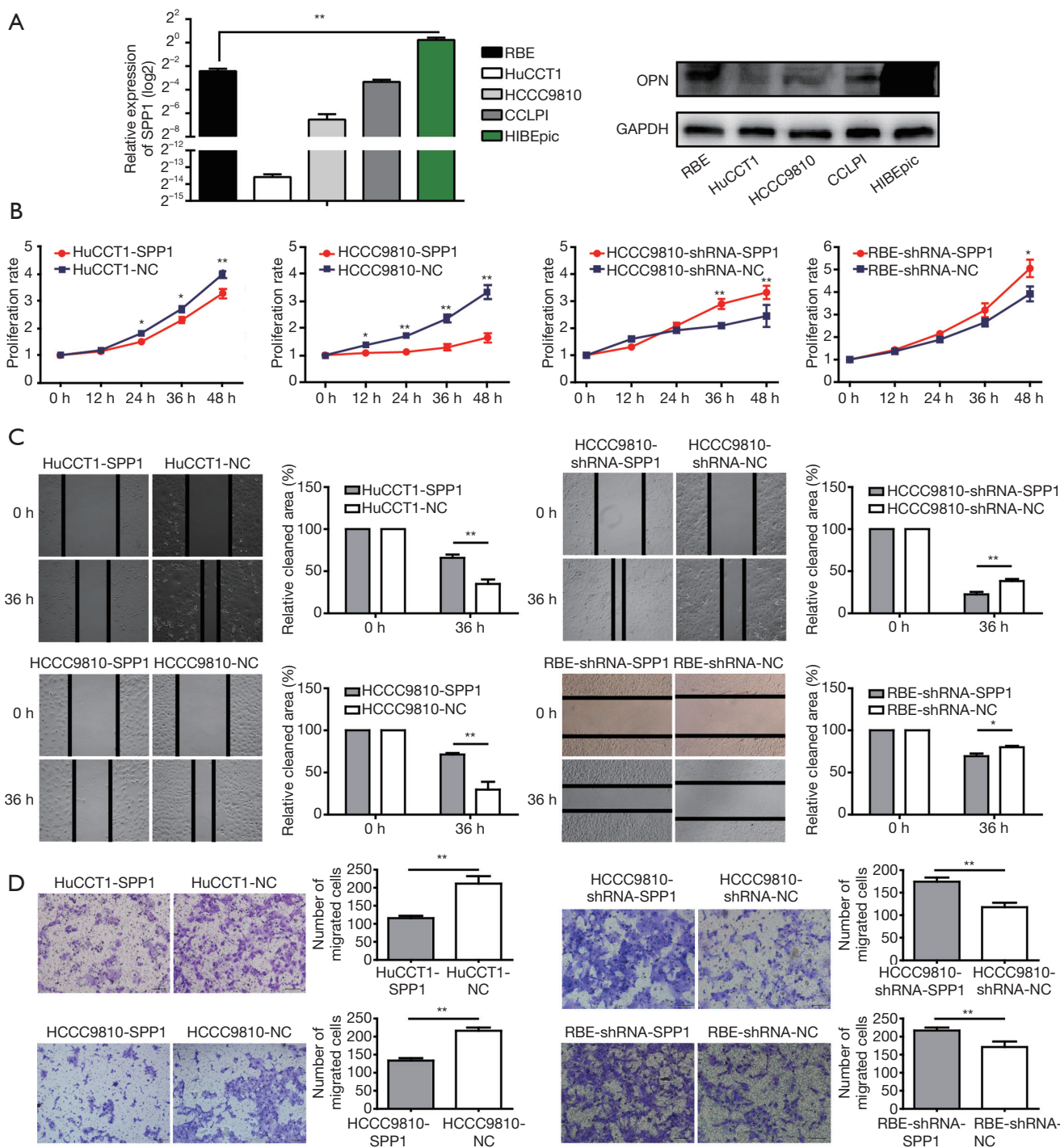
Figure 4 The biological function of OPN *in vitro*. (A) The expression level of SPP1-mRNA and OPN in cell lines of ICC (RBE, HuCCT1, HCCC9810, CCLPI) and intrahepatic bile duct (HIBEpic); (B) proliferation assay of constructed ICC cell lines. Proliferation accelerated in OPN up-regulated group and decelerated in OPN down-regulated group compared with their NC; (C) wound healing assay of OPN-regulated ICC cell lines. Up-regulation cell lines migrated faster than NC, while down-regulation cell lines migrated slower than the NC; (D) transwell invasion assay of gene-edited ICC cell lines. The number of the invaded cell was higher in OPN over-expressed cell lines and lower in OPN reduced cell line when compared with their NC respectively. (*, P<0.05, **, P<0.01). ICC, intrahepatic cholangiocarcinoma; OPN, osteopontin; NC, negative control.

592

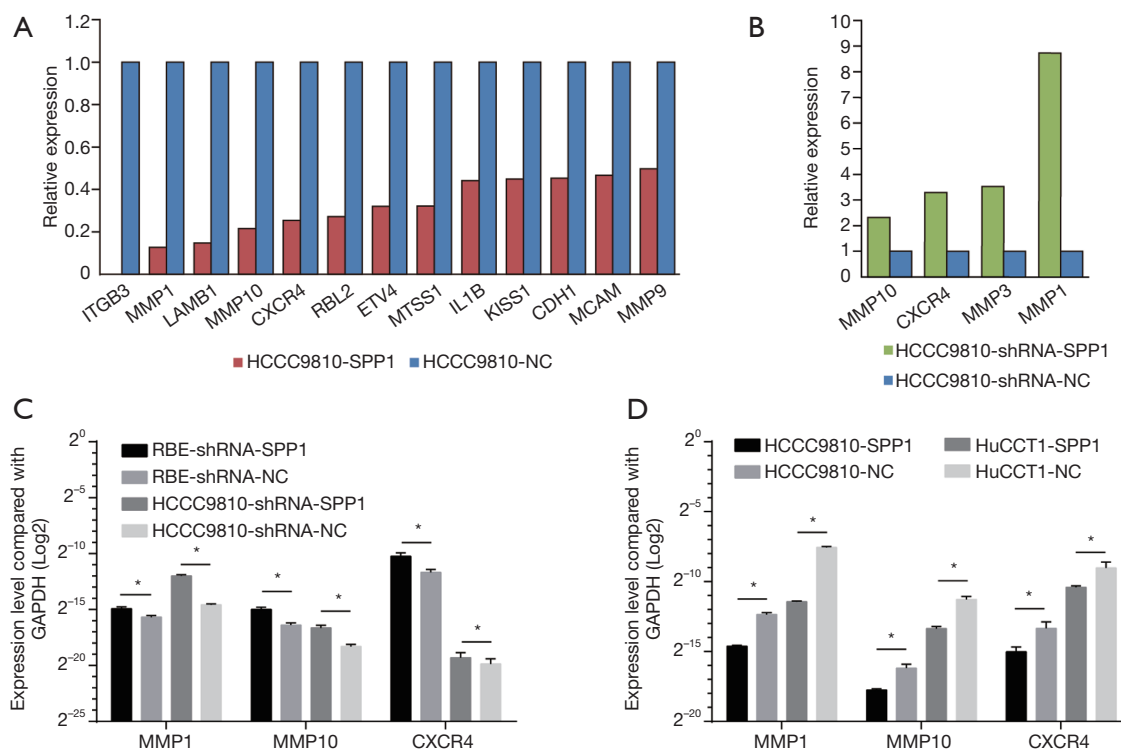Zhou et al. Circulating OPN/volume in ICC

Figure 5 Metastasis associated genes regulated by OPN. (A) Thirteen genes down-regulated in HCCC9810-SPP1 compared with HCCC9810-NC; (B) four up-regulated genes caused by OPN knock-down in HCCC9810; (A,B) relative expression was normalized to the controlled cell lines which equal to one; (C) validation of *MMP1*, *MMP10*, and *CXCR4* in OPN down-regulated ICC cell lines and their NCs; (D) validation of *MMP1*, *MMP10*, and *CXCR4* in OPN up-regulated ICC cell lines and their NC. *, P<0.05. NC, negative control; OPN, osteopontin; ICC, intrahepatic cholangiocarcinoma.

results which were its low expression being associated with lymph node metastasis and shorter OS. Functionally, over-expression of OPN inhibits phenotypes facilitating ICC metastasis by negatively regulating *MMP1*, *MMP10*, and *CXCR4*.

Circulating OPN/volume was able to provide information for the treatment strategy among resectable patients. Patients with a high level of OPN/volume had a better prognosis; they could benefit well from resection alone. Meanwhile, for those with low OPN/volume, the prognosis of surgery alone is unsatisfactory, and adjuvant chemotherapy is needed to improve long-term survival. Both fluoropyrimidine-base and gemcitabine-based chemotherapy are frequently adopted. Chemotherapy has been proven effective for unresectable patients with advanced or metastatic ICC, while the benefit of adjuvant chemotherapy remains unclear (33). Some studies reported that adjuvant chemotherapy had a survival advantage for patients with positive lymph node or positive margin (9,34).

However, there were also studies holding the opposing view that no survival benefit correlated with adjuvant chemotherapy (35). Our study revealed that adjuvant chemotherapy was beneficial for patients with a low level of OPN/volume, which could predict aggressive features and early recurrence, and not effective for those with a high level. Chemotherapy might kill or inhibit the micro tumor lesions which cannot be detected by conventional examination, thereby contributing to a survival benefit in patients with low OPN/volume.

Circulating OPN was positively correlated with tumor volume, while OPN in tissue was not. The finding confirmed the hypothesis raised by Loosen *et al.* (36) according to the evidence that both ICC parenchymal cell (24) and stromal cell (37) could express OPN. It also help explain the opposite prognostic value between serum OPN (36) and tissue OPN (22,23) to some extent. Considering that circulating OPN was mainly expressed by the tumor, circulating OPN might reflect the combined effect of tumor

volume and OPN function. Therefore, we calculated OPN per tumor volume to unify circulating and local index, so as to look into the intrinsic effect of OPN. By adjusting the confounding factor of tumor volume, OPN/volume seemed a more reasonable new indicator. Standardization of serum biomarker by volume was also used in other tumors. Compared with using AFP alone, AFP/volume seemed a better prognostic indicator for HCC patients (28,38). In well or intermediately differentiated prostate cancer, PSA/volume is the strongest predictor of tumor undergrading (39). In this study, a low level circulating OPN/volume was an indicator of metastatic behavior and poor survival, which coincided with the findings from local tissue. Two other studies by Terashi *et al.* (22) (n=73) and Iguchi *et al.* (23) (n=61) showed similar results in that decreased expression of OPN was associated with shorter survival time.

ICC cells expressing higher levels of OPN are more likely to resemble normal bile duct epithelial and have a lower degree of the malignant phenotype. The role of OPN in ICC still remains controversial. Although there were reports regarding OPN as a risk factor (24,36,37), our data indicated that OPN might function as a protective prognostic factor (22,23). The protective effect of OPN in liver pathogenesis has been reported. Plasma OPN levels were significantly elevated during acute liver injury, while very high levels of OPN were associated with good outcomes (40). In an ischemia-reperfusion mouse model, up regulation of OPN partially protected from hepatic injury and inflammation (41). In another mouse model of liver carcinogenesis induced by DEN, intracellular OPN (iOPN) negatively regulated toll-like receptor mediated immune responses to reduce pro-inflammatory cytokines, thus impeding hepatocarcinogenesis (42). Moreover, ICC in the OPN high expression group was better differentiated than that in the medium and low expression group. Another study also found that ICC expressed low levels of OPN irrespective of the tumor differentiation grade (43).

This study showed that *MMP10*, *CXCR4*, and *MMP1* were potential metastasis associated genes influenced by OPN. OPN might inhibit migration and invasion of ICC cell lines by down-regulating *MMP1*, *MMP10* and *CXCR4*. CXCR4 is a conserved chemokine receptor specific for SDF1 (also known as CXCL12) with strong chemotactic activity for lymphocytes (44). Lymph node metastasis associated with CXCR4/SDF1 has been found in breast cancer (45) and head and neck squamous cell carcinoma (46). Binding of SDF1 to CXCR4 induces invasion by activating downstream

pathways like PI3K (47), MAPK (48), and ERK1/2 (49). SDF1 is able to enhance the expression and the function of MMPs (50). MMP1 promotes lymph node metastasis in esophageal squamous cell carcinoma (ESCC) (51), and peritoneal dissemination in ovarian cancer (52). MMP10 was found through a data assessment to be correlated with metastatic behavior in many human cancer types (53). MMP1 (54) and MMP10 (55) also promote the formation of the pre-metastatic niche. The crosstalk between MMP10 and CXCR4/SDF1 axis stimulates cancer cell proliferation, angiogenesis, and metastasis (56).

There are some limitations to this study. First, we cannot deny the existence of biases caused by the retrospective study. The clinical value of circulating OPN/volume is in need of further validation in a prospective cohort, optimally in a multicenter study. Second, patients enrolled in this study were those who have undergone curative resection; thus, the findings may not be extended to patients with unresectable or recurrent lesions. Third, the biological function of OPN was preliminarily explored, and its mechanism still needs further study.

Conclusions

In summary, circulating OPN/volume was a protective prognostic factor for resectable ICC. Its low level indicated early recurrence, aggressive characteristics and poor survival in ICC patients before operation. OPN/volume also had a potential role in developing strategy of adjuvant therapy after curative resection. Functionally, OPN might inhibit migration and invasion of ICC cell lines by down-regulating *MMP1*, *MMP10*, and *CXCR4*.

Acknowledgments

Footnote

Conflicts of Interest: The authors have no conflicts of interest to declare.

Ethical Statement: This study was approved by the ethics committee at Zhongshan Hospital (No. B2018-018).

References

1. DeOliveira ML, Cunningham SC, Cameron JL, et al. Cholangiocarcinoma: thirty-one-year experience with 564 patients at a single institution. Ann Surg 2007;245:755-62.

2. Farges O, Fuks D, Le Treut YP, et al. AJCC 7th edition of TNM staging accurately discriminates outcomes of patients with resectable intrahepatic cholangiocarcinoma: By the AFC-IHCC-2009 study group. Cancer 2011;117:2170-7.

3. Khan SA, Emadossadaty S, Ladep NG, et al. Rising trends in cholangiocarcinoma: is the ICD classification system misleading us? J Hepatol 2012;56:848-54.

4. McLean L, Patel T. Racial and ethnic variations in the epidemiology of intrahepatic cholangiocarcinoma in the United States. Liver Int 2006;26:1047-53.

5. Taylor-Robinson SD, Toledano MB, Arora S, et al. Increase in mortality rates from intrahepatic cholangiocarcinoma in England and Wales 1968-1998. Gut 2001;48:816-20.

6. Patel T. Worldwide trends in mortality from biliary tract malignancies. BMC Cancer 2002;2:10.

7. Patel T. Increasing incidence and mortality of primary intrahepatic cholangiocarcinoma in the United States. Hepatology 2001;33:1353-7.

8. Saxena A, Chua TC, Sarkar A, et al. Clinicopathologic and treatment-related factors influencing recurrence and survival after hepatic resection of intrahepatic cholangiocarcinoma: a 19-year experience from an established Australian hepatobiliary unit. J Gastrointest Surg 2010;14:1128-38.

9. Sur MD, In H, Sharpe SM, et al. Defining the Benefit of Adjuvant Therapy Following Resection for Intrahepatic Cholangiocarcinoma. Ann Surg Oncol 2015;22:2209-17.

10. Marubashi S, Gotoh K, Takahashi H, et al. Prediction of the postoperative prognosis of intrahepatic cholangiocarcinoma (ICC): importance of preoperatively-determined anatomic invasion level and number of tumors. Dig Dis Sci 2014;59:201-13.

11. Tabrizian P, Jibara G, Hechtman JF, et al. Outcomes following resection of intrahepatic cholangiocarcinoma. HPB (Oxford) 2015;17:344-51.

12. Ghiassi-Nejad Z, Tarchi P, Moshier E, et al. Prognostic Factors and Patterns of Locoregional Failure After Surgical Resection in Patients With Cholangiocarcinoma Without Adjuvant Radiation Therapy: Optimal Field Design for Adjuvant Radiation Therapy. Int J Radiat Oncol Biol Phys 2017;99:805-11.

13. Zhang H, Yang T, Wu M, et al. Intrahepatic cholangiocarcinoma: Epidemiology, risk factors, diagnosis and surgical management. Cancer Lett 2016;379:198-205.

14. Luo X, Yuan L, Wang Y, et al. Survival outcomes and prognostic factors of surgical therapy for all potentially resectable intrahepatic cholangiocarcinoma: a large single-center cohort study. J Gastrointest Surg 2014;18:562-72.

15. Uchiyama K, Yamamoto M, Yamaue H, et al. Impact of nodal involvement on surgical outcomes of intrahepatic cholangiocarcinoma: a multicenter analysis by the Study Group for Hepatic Surgery of the Japanese Society of Hepato-Biliary-Pancreatic Surgery. J Hepatobiliary Pancreat Sci 2011;18:443-52.

16. Deng B, Zhang XF, Zhu XC, et al. Correlation and prognostic value of osteopontin and Bcl-2 in hepatocellular carcinoma patients after curative resection. Oncol Rep 2013;30:2795-803.

17. Chen RX, Xia YH, Xue TC, et al. Osteopontin promotes hepatocellular carcinoma invasion by up-regulating MMP-2 and uPA expression. Mol Biol Rep 2011;38:3671-7.

18. Cao L, Fan X, Jing W, et al. Osteopontin promotes a cancer stem cell-like phenotype in hepatocellular carcinoma cells via an integrin-NF-kappaB-HIF-1alpha pathway. Oncotarget 2015;6:6627-40.

19. Dong Q, Zhu X, Dai C, et al. Osteopontin promotes epithelial-mesenchymal transition of hepatocellular carcinoma through regulating vimentin. Oncotarget 2016;7:12997-3012.

20. Iqbal J, McRae S, Banaudha K, et al. Mechanism of hepatitis C virus (HCV)-induced osteopontin and its role in epithelial to mesenchymal transition of hepatocytes. J Biol Chem 2013;288:36994-7009.

21. Iqbal J, McRae S, Mai T, et al. Role of hepatitis C virus induced osteopontin in epithelial to mesenchymal transition, migration and invasion of hepatocytes. PLoS One 2014;9:e87464.

22. Terashi T, Aishima S, Taguchi K, et al. Decreased expression of osteopontin is related to tumor aggressiveness and clinical outcome of intrahepatic cholangiocarcinoma. Liver International 2004;24:38-45.

23. Iguchi T, Yamashita N, Aishima S, et al. A comprehensive analysis of immunohistochemical studies in intrahepatic cholangiocarcinoma using the survival tree model.

Oncology 2009;76:293-300.

24. Zheng Y, Zhou C, Yu X, et al. Osteopontin promotes metastasis of intrahepatic cholangiocarcinoma through recruiting MAPK1 and mediating Ser675 phosphorylation of β-Catenin. Cell Death Dis 2018;9:179.

25. Spandidos A, Wang X, Wang H, et al. PrimerBank: a resource of human and mouse PCR primer pairs for gene expression detection and quantification. Nucleic Acids Res 2010;38:D792-9.

26. Rao SX, Lambregts DM, Schnerr RS, et al. CT texture analysis in colorectal liver metastases: A better way than size and volume measurements to assess response to chemotherapy? United European Gastroenterol J 2016;4:257-63.

27. Hsu CY, Huang YH, Hsia CY, et al. A new prognostic model for hepatocellular carcinoma based on total tumor volume: the Taipei Integrated Scoring System. J Hepatol 2010;53:108-17.

28. Sharma Y, Weaver MJ, Ludwig DR, et al. Serum alpha-fetoprotein level per total tumor volume as a predictor of recurrence of hepatocellular carcinoma after resection. Surgery 2018;163:1002-7.

29. Gao Q, Qiu SJ, Fan J, et al. Intratumoral balance of regulatory and cytotoxic T cells is associated with prognosis of hepatocellular carcinoma after resection. J Clin Oncol 2007;25:2586-93.

30. Lin CK, Tsai WC, Lin YC, et al. Osteopontin predicts the behaviour of atypical meningioma. Histopathology 2012;60:320-5.

31. Zhang XF, Beal EW, Bagante F, et al. Early versus late recurrence of intrahepatic cholangiocarcinoma after resection with curative intent. Br J Surg 2018;105:848-56.

32. Aloia TM, Taouli B, Rubbia-Brandt L, et al. Intrahepatic Bile Ducts. In: Amin MB, Edge S, Greene F, et al. Editors. AJCC Cancer Staging Manual. 8th edition. New York: Springer International Publishing, 2017:299.

33. Valle J, Wasan H, Palmer DH, et al. Cisplatin plus gemcitabine versus gemcitabine for biliary tract cancer. N Engl J Med 2010;362:1273-81.

34. McNamara MG, Walter T, Horgan AM, et al. Outcome of adjuvant therapy in biliary tract cancers. Am J Clin Oncol 2015;38:382-7.

35. Tran Cao HS, Zhang Q, Sada YH, et al. The role of surgery and adjuvant therapy in lymph node-positive cancers of the gallbladder and intrahepatic bile ducts. Cancer 2018;124:74-83.

36. Loosen SH, Roderburg C, Kauertz KL, et al. Elevated levels of circulating osteopontin are associated with a poor survival after resection of cholangiocarcinoma. J Hepatol 2017;67:749-57.

37. Sulpice L, Rayar M, Desille M, et al. Molecular Profiling of Stroma Identifies Osteopontin as an Independent Predictor of Poor Prognosis in Intrahepatic Cholangiocarcinoma. Hepatology 2013;58:1992-2000.

38. Furihata T, Sawada T, Kita J, et al. Serum alpha-fetoprotein level per tumor volume reflects prognosis in patients with hepatocellular carcinoma after curative hepatectomy. Hepatogastroenterology 2008;55:1705-9.

39. Corcoran NM, Casey RG, Hong MK, et al. The ability of prostate-specific antigen (PSA) density to predict an upgrade in Gleason score between initial prostate biopsy and prostatectomy diminishes with increasing tumour grade due to reduced PSA secretion per unit tumour volume. BJU Int 2012;110:36-42.

40. Srungaram P, Rule JA, Yuan HJ, et al. Plasma osteopontin in acute liver failure. Cytokine 2015;73:270-6.

41. Patouraux S, Rousseau D, Rubio A, et al. Osteopontin deficiency aggravates hepatic injury induced by ischemia-reperfusion in mice. Cell Death Dis 2014;5:e1208.

42. Fan X, He C, Jing W, et al. Intracellular Osteopontin inhibits toll-like receptor signaling and impedes liver carcinogenesis. Cancer Res 2015;75:86-97.

43. Demarez C, Hubert C, Sempoux C, et al. Expression of Molecular Differentiation Markers Does Not Correlate with Histological Differentiation Grade in Intrahepatic Cholangiocarcinoma. PLoS One 2016;11:e0157140.

44. Oberlin E, Amara A, Bachelerie F, et al. The CXC chemokine SDF-1 is the ligand for LESTR/fusin and prevents infection by T-cell-line-adapted HIV-1. Nature 1996;382:833-5.

45. Peng SB, Zhang X, Paul D, et al. Identification of LY2510924, a novel cyclic peptide CXCR4 antagonist that exhibits antitumor activities in solid tumor and breast cancer metastatic models. Mol Cancer Ther 2015;14:480-90.

46. Nakamura T, Shinriki S, Jono H, et al. Intrinsic TGF-beta2-triggered SDF-1-CXCR4 signaling axis is crucial for drug resistance and a slow-cycling state in bone marrow-disseminated tumor cells. Oncotarget 2015;6:1008-19.

47. Leelawat K, Leelawat S, Narong S, et al. Roles of the MEK1/2 and AKT pathways in CXCL12/CXCR4 induced cholangiocarcinoma cell invasion. World J Gastroenterol 2007;13:1561-8.

48. Barbero S, Bonavia R, Bajetto A, et al. Stromal cell-derived factor 1alpha stimulates human glioblastoma cell growth through the activation of both extracellular signal-regulated kinases 1/2 and Akt. Cancer Res 2003;63:1969-74.

49. Liao YX, Fu ZZ, Zhou CH, et al. AMD3100 reduces CXCR4-mediated survival and metastasis of osteosarcoma by inhibiting JNK and Akt, but not p38 or Erk1/2, pathways in in vitro and mouse experiments. Oncol Rep 2015;34:33-42.

50. Janowska-Wieczorek A, Marquez LA, Dobrowsky A, et al. Differential MMP and TIMP production by human marrow and peripheral blood CD34(+) cells in response to chemokines. Exp Hematol 2000;28:1274-85.

51. Liu M, Hu Y, Zhang MF, et al. MMP1 promotes tumor growth and metastasis in esophageal squamous cell carcinoma. Cancer Lett 2016;377:97-104.

52. Yokoi A, Yoshioka Y, Yamamoto Y, et al. Malignant extracellular vesicles carrying MMP1 mRNA facilitate peritoneal dissemination in ovarian cancer. Nat Commun 2017;8:14470.

53. Justilien V, Regala RP, Tseng IC, et al. Matrix metalloproteinase-10 is required for lung cancer stem cell maintenance, tumor initiation and metastatic potential. PLoS One 2012;7:e35040.

54. Lu X, Wang Q, Hu G, et al. ADAMTS1 and MMP1 proteolytically engage EGF-like ligands in an osteolytic signaling cascade for bone metastasis. Genes Dev 2009;23:1882-94.

55. Huang Y, Song N, Ding Y, et al. Pulmonary vascular destabilization in the premetastatic phase facilitates lung metastasis. Cancer Res 2009;69:7529-37.

56. Garcia-Irigoyen O, Latasa MU, Carotti S, et al. Matrix metalloproteinase 10 contributes to hepatocarcinogenesis in a novel crosstalk with the stromal derived factor 1/C-X-C chemokine receptor 4 axis. Hepatology 2015;62:166-78.